Comparison of the ultrafast hot electron dynamics of titanium nitride and gold for plasmonic applications

Brock Doiron[A], Yi Li[A], Andrei P. Mihai[B], Lesley F. Cohen[A], Peter K. Pretrov[B], Neil M. Alford[B], Rupert F. Oulton[A], Stefan A. Maier[A]
[A] Department of Physics, Imperial College London, London, UK
[B] Department of Materials, Imperial College London, London, UK

ABSTRACT

With similar optical properties to gold and high thermal stability, titanium nitride continues to prove itself as a promising plasmonic material for high-temperature applications in the visible and near-infrared. In this work, we use transient pump probe differential reflection measurements to compare the electron energy decay channels in titanium nitride and gold thin films. Using an extended two temperature model to incorporate the photoexcited electrons, it is possible to separate the electron-electron and electron-phonon scattering contributions immediately following the arrival of the pump pulse. This model allows for incredibly accurate determination of the internal electronic properties using only optical measurements. As the electronic properties are key in hot electron applications, we show that titanium nitide has substantially longer electron thermalization and electron-phonon scattering times. With this, we were also able to resolve electron thermal conduction in the film using purely optical measurements.

Keywords: Titanium nitride, plasmonics, electron dynamics, hot electrons

1. INTRODUCTION

Titanium nitride's thermal stability and comparable optical properties to gold have proven beneficial for plasmonics where high-temperature operation is essential. One intriguing opportunity is in so-called hot-carrier applications where the heating loss of plasmonics is circumvented by utilizing the energetic electrons before they thermalize with the lattice. Following photon absorption or the nonradiative decay of a surface plasmon, an electron-hole pair is generated in the material. If one of these charge carriers is sufficiently far from the Fermi level, it is termed a hot-carrier. This hot electron or hot hole then has the potential to be extracted via a Schottky barrier with a semiconductor or participate in a chemical reaction with a molecule in contact with the metal. This has been of great use in photocatalysis and photovoltaics where these energetic electrons are transferred to an adjacent material on these ultrashort timescales. Titanium nitride has been used in such applications, where the intrinsic absorption properties were used to generate hot-carriers using visible light that were then extracted across an Ohmic junction[1]. In addition, colloidal TiN has also been used for solar water splitting with plasmonically-generated hot eletrons[2]. However, hot carriers are only useful for a limited time as their energy is lost via electron-electron and electron-phonon interactions. Thus, to understand the practicality of using these energetic carriers for productive purposes, it is critical to characterize the temporal dynamics of hot carriers and understand the subsequent energy loss channels. Although the physics of the processes involved has been studied extensively in the past several decades, it is relevant to revisit this to provide a foundation for the use of plasmonics in hot electron applications and determine how novel materials can play a role in the development of commercially-viable plasmonic devices. In this work, we introduce a theoretical framework in which the internal electron dynamics can be well-understood in relation to the the relative temperatures of the interacting electron and phonon systems. To measure the transient changes in electron energy, we use time-resolved pump probe differential reflectivity measurements to examine the evolution of the electron system following excitation with sub-picosecond laser pulses. With the model presented, we are able to use these measurements to independently monitor the behaviour of phonon system as well as the photo-excited and thermal electron populations and the time scales in which they retain the energy absorbed from the laser pulse. In this work, we find that electron and phonon scattering processes in titanium nitride are considerably slower than in gold, suggesting their suitability for hot-electron applications.

2. THEORY AND MODELLING

Upon absorption of a femtosecond laser pulse, the electron distribution is perturbed to a non-Fermi distribution, determined by the pulse energy and density of states of the material[3-4]. In an energy range close to the Fermi level, $|E - E_F| < k_b T$, this can be represented as the sum of a thermal electron (ie. Fermi) distribution and an approximately constant nonthermal component[5] to represent the photoexcited electrons. Immediately following the laser pulse, this can be written as:

$$f(E, t = 0) = f_{NT}(t = 0) + f_T(t = 0) = f_0 + \left[\exp\left(-\frac{E - E_F}{k_b T_0}\right) + 1\right]^{-1}$$

The excess energy in the nonthermal electrons is subsequently distributed amongst the thermal electrons via electron-electron scattering events, which occur on the order of tens of femtosecond. This results in the heating of the thermal electron population and decay of the nonthermal component until the total electron distribution reaches an elevated-temperature Fermi-Dirac distribution with a well-defined total temperature, T_e. The decay of the nonthermal electron distribution is described by Fermi liquid theory[3] using a thermalization time, τ_{Th}, in terms of the energy difference from the Fermi level $\delta E = E - E_F$:

$$\tau_{Th}(E) = \frac{128}{\pi^2 \sqrt{3} \omega_p} \left(\frac{E_F}{\delta E}\right)^2$$

where ω_p is the plasma frequency and and E_F the Fermi energy. This suggests that the thermalization time scales quadratically with increasing energy separation from the Fermi level, with higher energy electrons decaying faster. This results in a time-dependent electron distribution as follows[5]:

$$f(E, t) = f_{NT}(t) + f_T(t) = f_0 \exp\left(-\frac{t}{\tau_{Th}}\right) + \left[\exp\left(-\frac{E - E_F}{k_b T_E(t)}\right) + 1\right]^{-1}$$

The temporal evolution of the thermal electron system is described using an extended two-temperature model[6]. Three interacting thermal bodies are considered: nonthermal electrons, thermal electrons and phonons. The evolution is described by the following three coupled differential equations:

$$\frac{\partial N}{\partial t} = -\alpha N$$
$$C_e \frac{\partial T_e}{\partial t} = \alpha N - \nabla \cdot (\kappa_e \nabla T_l) - G(T_e - T_l)$$
$$C_l \frac{\partial T_l}{\partial t} = G(T_e - T_l) - \nabla \cdot \left(\kappa_p \nabla T_l\right)$$

The nonthermal electron distribution is repesented by energy density, N, which characterizes the initial energy absorbed by the material from the laser pulse. These heat the thermal electrons via electron-electron interactions at a rate quantified by α, the electron gas heating rate. The energy of the thermal electrons is described by the electron temperature T_e corresponding to the Fermi-Dirac distribution, whose temperature change is modulated by the electron heat capacity, C_e. The thermal electron population loses energy via two channels, the first being thermal diffusion via charge carriers. Following the heating of the thermal population, there remains an electron temperature gradient, as a result, heat is conducted away from the laser spot with associated carrier thermal conductivity, κ_e. The second loss channel is scattering with phonons, which has associated coupling parameter, G. This results in heating of the phonon system, described by a temperature T_l, which is modulated by the lattice heat capacity, C_l. The only channel for the phonons to lose energy is thermal conduction via phonons due to the lattice temperature gradient ∇T_l, occurring with lattice thermal conductivity κ_p.

In this work, the critical parameters to extract are the lifetimes, which describe the length of time energy remains in each of the three thermal systems. As described above, the decay of the nonthermal electron system is described by a thermalization time, which can be related to the electron gas heating rate by $\tau_{th} = \alpha^{-1}$. Neglecting the electron thermal conduction due to the limited mean free path in metals[7-8], the following decay of the thermal electron energy is dominated by electron-phonon scattering. When taking the difference of the last two equations, the remaining system resembles a two-body Newton cooling problem, characterized by an electron-phonon lifetime $\tau_{ep}^{-1} \approx G\left(\frac{1}{C_e} + \frac{1}{C_l}\right)$. This energy exchange continues until the electron and lattice temperatures approach an equilibrium value where the process is then bottlenecked. Following this, the electrons can only cool at a rate equal to the phonon-phonon scattering rate away from the excited area due to the temperature gradient, ∇T_l. On these longer time scales, it is observed as a change in the exponential that follows the phonon-phonon scattering lifetime, τ_{pp}, related to the thermal conductivity of the material. These processes are summarized in Figure 1, showing the temporal evolution of the temperatures of the three thermal bodies in question. With such a model, it is now possible to independently monitor the response of the electrons and phonons to a femtosecond laser pulse even in the regime where electron heating and cooling processes are competing.

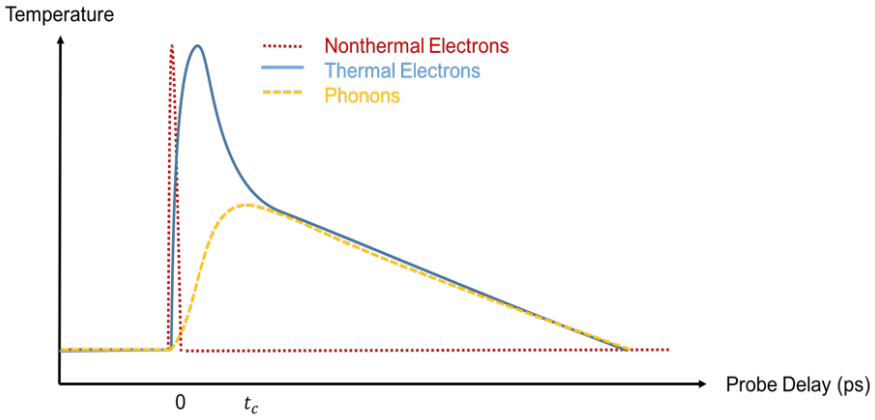

Figure 1. Schematic diagram of the treatment of the three interacting thermal bodies (nonthermal electrons, electrons, phonons) in the extended two temperature model used in this work.

3. RESULTS

3.1 Experimental Setup and Parameter Extraction

Following the disturbance of the electron energy distribution caused by the laser pulse, there is a small change in absorptive properties of the material until equilibrium is achieved. To measure these dynamics, we use time-resolved pump probe differential reflectivity measurements using 150 fs pulses from a Chameleon Ultra II Ti:Sapphire laser. A pump pulse (850nm) at 2mW focused to 10 μm-diameter is used to disturb the electron distribution and a delayed low-energy probe pulse (1150nm) generated using an optical parametric oscillator (OPO) is used to monitor the relaxation dynamics in titanium nitride and gold up to several hundred picoseconds after pump excitation. Through monitoring the differential reflectivity of the probe, it is possible to estimate the electron and phonon lifetimes as outlined in the model above. As the nonthermal electron distribution thermalizes with the thermal electron system, higher energy states become occupied, inhibiting absorption of the probe pulse. This is observable by a rapid initial increase in the reflected signal following the temporal overlap of the pump and probe beams ($t = 0$). The reflectivity returns toward its initial value as the electron system returns to its equilibrium state. This is fitted using a Levenberg Marquardt algorithm[9] to a phenomenological solution to the two temperature model where the interaction times are described by lifetimes: τ_{Th}, τ_{ep}, and τ_{pp}. Shown in Figure 2 are two exemplary measurements of a 60nm titanium nitride and gold film on a silica substrate fitted using the extended two temperature model with adjusted R^2 values of 0.959 and 0.973 for titanium and gold respectively. This allows for unprecedented accuracy in the determination of the three lifetimes.

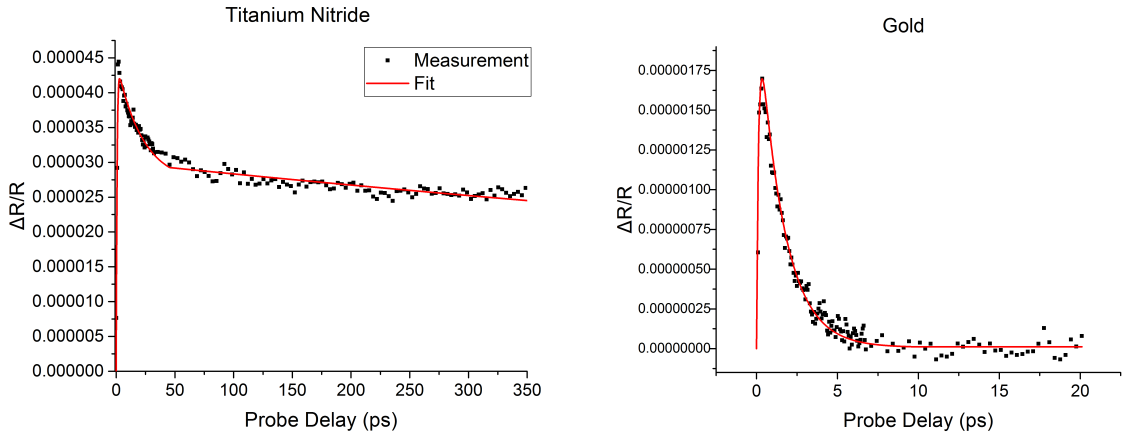

Figure 2. Pump-probe differential reflectivity measurements (black) of titanium nitride and gold films fitted to the extended two temperature model (red).

3.2 Titanium Nitride for Hot Electron Applications

To investigate the vability of a novel material for hot electron applications, it is imperative to compare it to a well-known control. In our case, gold is used due to the similarity of the optical properties as well as the prevalence of gold in the literature of plasmonic hot electron studies[10-11]. It is immediately apparent in Figure 1 that the differential reflectivity signal is nonzero in titanium nitride for hundreds of picoseconds whereas gold returns to equilibrium within ten picoseconds following laser absorption. Figure 2 shows the two plots in Figure 1 normalized to their respective maximum measured value to allow for a direct comparison between the two plots. As was previously discovered[12], titanium nitride has an electron-phonon lifetime an order of magnitude larger than in gold. With the fit shown, it was determined to be $19.5 \pm 1.8\ ps$ for titanium nitride and $1.52 \pm 0.04\ ps$ in gold. Furthermore, the slower rise time of the differential reflectivity of titanium nitride is clearly visible associated with electron thermalization times of $870 \pm 60\ fs$ and $140 \pm 10\ fs$ for titanium nitide and gold respectively. The longer lifetimes in titanium nitride make it an ideal platform to investigate the role of the initial nonthermal population on the subsequent electron energy processes. As is exemplified in Figure 2, the experimental data for titanium nitride rises above the peak numerical fitting for several hundred femtoseconds. We attribute this to thermal diffusion of electrons into the titanium nitride, since the film's thickness is greater than the penetration depth of the field. As a result, the electrons are only initially heated at the surface of the material estabilishing a temperature gradient normal to the surface. Although this has been predicted theoretically[13], this has yet to be observed in a plasmonic material using pump-probe measurements. The slow response of TiN, makes this phenomenon clearly visible in experimental data.

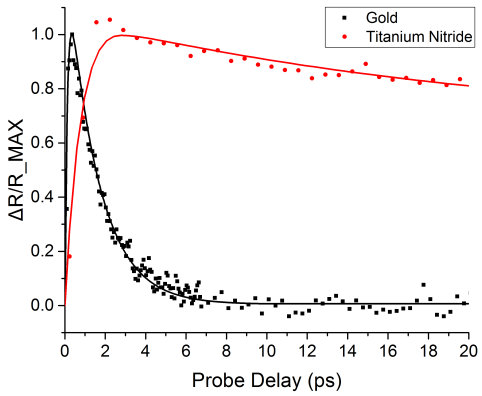

Figure 3. Differential reflection measurements normalized to the maximum measured value to exemplify the slow electron-electron and electron-phonon scattering in titanium nitride.

4. CONCLUSION

We have presented a theoretical framework for characterizing the electron and phonon dynamics using changes in the reflectivity on ultrafast timescales via an extended two temperature model which includes the energy distribution of the nonthermal distribution. Equipped with this, it was possible to investigate the differences between titanium nitride and gold in the context of developing commercially-viable plasmonic hot electron applications using pump-probe differential reflectivity measurements using ultrashort laser pulses. With the incredibly accurate fitting to the model, the relevant electron lifetimes were determined with a relative error of less than 10% for all measurements. As such, we are able to conclude that with the longer electron thermalization and electron-phonon lifetimes of titanium nitride suggest more efficient hot carrier extraction as the enegetic electrons remain for almost an order of magnitude longer than in gold, which is conventionally used. With all lifetimes longer in titanium nitride, we will continue to look at the effect of the initial nonthermal distribution on the subsequent energy relaxation processes in both titanium nitride films and nanostructures.

REFERENCES

[1] Ishii, S., Shinde, S. L., Jevasuwan, W., Fukata, N. and Nagao, T., "Hot electron excitation using visible light," ACS Photonics 3(9), 1552-1557 (2016).

[2] Naldoni, A., Guler, U., Wang, W., Marelli, M., Malara, F., Meng, X., Besteiro, L. V., Govorov A. O., Kildishev, A. V., Boltasseva, A. and V. M. Shalaev, V. M., "Broadband hot electron collection for solar water splitting with plasmonic titanium nitride," Adv. Opt. Mat. 1601031 (2017).

[3] Giri, A. and Hopkins, P. E., "Transient thermal and nonthermal electron and phonon relaxation after short-pulsed laser heating of metals" J. Appl. Phys. 118, 215101 (2015).

[4] Groeneveld, R. H. M., Sprik, R. and Lagendijk, A., "Effect of a nonthermal electron distribution on the electron-phonon energy relaxation process in noble metals" Phys. Rev. B 45(9), 5079-5082 (1992).

[5] Fann, W. S., Storz, R., Tom H. W. K. and Bokor, J., "Electron thermalization in gold" Phys. Rev. B 46(20), 13592-13595 (1992).

[6] Sun, C.-K., Vallée, F., Acioli, L. H., Ippen, E. P. and Fujimoto, J. G., "Femtosecond-tunable measurement of electron thermalization in gold" Phys. Rev. B 50(20), 15337-15348 (1994).

[7] Gall, D., "Electron mean free path in elemental metals" J. Appl. Phys. 119, 085101 (2016).

[8] Chawls, J. S., Zhang, X. Y. and Gall, D., "Effective electron mean free path in TiN(001)" J. Appl. Phys. 113, 063704 (2013).

[9] Pujol, J., "The solution of nonlinear inverse problems and the Levenberg-Marquardt method" Geophysics, 72(4), W1-W16 (2007).

[10] Reineck, P., Brick, D., Mulvaney, P. and Bach, U., "Plasmonic hot electron solar cells: The effect of nanoparticle size on quantum efficiency" J. Phys. Chem. Lett. 7(20), 4137-4141 (2016).

[11] Clavero, C., "Plasmon-induced hot-electron generation at nanoparticle/metal-oxide interfaces for photovoltaic and photocatalytics devices" Nat. Phot. 8, 95-103 (2014).

[12] Ferguson, H., Guler, U., Kinsey, N., Shalaev, V. M., Norris, T. B., and Boltasseva, A., "Hot electron relaxation in thin titanium nitride films," CLEO Proceedings, OSA Technical Digest (online) (2016).

[13] Qui, T. Q. and Tien, C. L., "Heat transfer mechanisms during short-pulse laser heating of metals" J. Heat Transfer 115(4), 835-841 (1993).